

Vibrational dynamics of aniline(Ar)₁ and aniline(CH₄)₁ clusters

M. R. Nimlos, M. A. Young, E. R. Bernstein, and D. F. Kelley

Citation: *The Journal of Chemical Physics* **91**, 5268 (1989); doi: 10.1063/1.457572

View online: <http://dx.doi.org/10.1063/1.457572>

View Table of Contents: <http://aip.scitation.org/toc/jcp/91/9>

Published by the *American Institute of Physics*



**COMPLETELY
REDESIGNED!**



**PHYSICS
TODAY**

Physics Today Buyer's Guide
Search with a purpose.

Vibrational dynamics of aniline(Ar)₁ and aniline(CH₄)₁ clusters

M. R. Nimlos,^{a)} M. A. Young,^{b)} E. R. Bernstein, and D. F. Kelley
Department of Chemistry, Colorado State University, Fort Collins, Colorado 80523

(Received 23 May 1989; accepted 18 July 1989)

The first excited electronic state (S_1) vibrational dynamics of aniline(Ar)₁ and aniline(CH₄)₁ van der Waals (vdW) clusters have been studied using molecular jet and time resolved emission spectroscopic techniques. The rates of intramolecular vibrational energy redistribution (IVR) and vibrational predissociation (VP) as functions of vibrational energy are reported for both clusters. For vibrational energy in excess of the cluster binding energy, both clusters are observed to dissociate. The dispersed emission spectra of these clusters demonstrate that aniline(Ar)₁ dissociates to all energetically accessible bare molecule states and that aniline(CH₄)₁ dissociates selectively to only the bare molecule vibrationless state. The emission kinetics show that in the aniline(Ar)₁ case, the initially excited states have nanosecond lifetimes, and intermediate cluster states have very short lifetimes. In contrast, the initially excited aniline(CH₄)₁ states and other intermediate vibrationally excited cluster states are very short lived (< 100 ps), and the intermediate cluster 0^0 state is observed. These results can be understood semiquantitatively in terms of an overall serial IVR/VP mechanism which consists of the following: (1) the rates of chromophore to vdW mode IVR are given by Fermi's golden rule, and the density of vdW vibrational states is the most important factor in determining the relative [aniline(Ar)₁ vs aniline(CH₄)₁] rates of IVR; (2) IVR among the vdW modes is rapid; and (3) VP rates can be calculated by a restricted vdW mode phase space Rice-Ramsberger-Kassel-Marcus theory. Since the density of vdW states is three orders of magnitude greater for aniline(CH₄)₁ than aniline(Ar)₁ at 700 cm^{-1} , the model predicts that IVR is slow and rate limiting in aniline(Ar)₁, whereas VP is slow and rate limiting in aniline(CH₄)₁. The agreement of these predictions with the experimental results is very good and is discussed in detail.

I. INTRODUCTION

Photoinduced unimolecular decomposition reactions are among the simplest reactions which can be studied experimentally and theoretically. One such reaction which has received considerable attention is the vibrational predissociation of small, isolated van der Waals (vdW) clusters for which one molecule is a chromophore and the other is a small "solvent" molecule. The cluster is excited by absorption of a photon to an oscillator strength bearing, nonstationary (zero order) cluster state. Such states are a coherent superposition of available cluster eigenstates and closely resemble chromophore vibronic states. Two dynamical events may transpire in such a system following the initial photoexcitation to S_1 vibronic levels: vibrational energy may be redistributed to modes other than the optically accessed zero order chromophore states; and at sufficient energies the cluster may dissociate. The fundamental theoretical understanding of these two kinetic processes should be accessible in terms of Fermi's golden rule¹ and unimolecular reaction rate² concepts.

Two theoretical models have been put forward to explain the dynamics of IVR and VP processes, and most of the available data has been interpreted in terms of one or the other of these models. These models treat IVR and VP to be

either "parallel" or "serial" processes. The Beswick-Jortner³ model considers dissociation to be a process which occurs in parallel with IVR. This treatment considers the direct coupling between the chromophore vibrational states of the bound complex and the plane wave states of a dissociated complex, and is most appropriate when the amount of energy put in vdW modes by a one quanta change in the chromophore mode is large compared to the binding energy. Under these high energy, weak binding conditions cluster dissociation occurs in one-half of a vibrational period when one vibrational chromophore quantum of energy is transferred into the vdW modes. As a result, IVR/VP occurs directly into the "dissociative continuum." This model is appropriate to diatomic(He)₁-type systems.

The above rather extreme conditions are not met in polyatomic clusters such as chromophore(X)₁, in which the chromophore is an aromatic molecule and X = Ar, CH₄, etc. In these polyatomic clusters, the binding energy is typically large compared to the separations of chromophore vibrational energy levels. Thus for polyatomic clusters, the Beswick-Jortner treatment seems inappropriate and is directly at odds with the more conventional serial model based on Rice-Ramsberger-Kassel-Marcus (RRKM) unimolecular reaction rate theory that we have put forth.^{2(b)}

In the serial model for the IVR/VP processes,^{2(b)} the vibrational phase space of the cluster is divided into two regions; the chromophore and the vdW regions. The rationale behind this partitioning of phase space is twofold: (1) an energy mismatch exists between the vdW modes (typically less than $\sim 50\text{ cm}^{-1}$) and the chromophore

^{a)} Current address: Solar Energy Research Institute, 1617 Cole Blvd., Golden, Colorado 80401.

^{b)} Current address: Department of Chemistry, University of California, Berkeley, California 94720.

modes (typically greater than $\sim 200 \text{ cm}^{-1}$); and (2) the coupling between these two sets of modes is small. Optical excitation typically puts most or all of the vibrational energy into the chromophore phase space region. The amount of energy in the vdW modes then increases as chromophore to vdW mode IVR proceeds. With the assumption that IVR among the van der Waals modes is very rapid, the VP rate can be calculated by a restricted (to the vdW vibrational phase space) RRKM theory^{2(a)} in which the unimolecular cluster dissociation rate constant depends only upon the total amount of energy in vdW modes. Therefore, in this latter model, VP can occur only after chromophore to the vdW mode IVR has occurred; the rate depends upon the amount of energy in vdW modes and this energy varies with time, due to chromophore to vdW mode IVR.

The two theoretical models, parallel and serial IVR/VP processes, predict much different appearance kinetics of individual vibronic states of solute/solvent clusters. The question of serial *vs* parallel processes for vibronic dynamics can in many cases be unambiguously answered by time resolved studies. In the absence of temporal resolution, assumptions of only parallel or only serial relaxation processes are made for the data interpretation.

Several static spectroscopic studies on polyatomic vdW clusters have been reported⁴⁻¹¹ and a number of review articles summarize those results.¹² In most of these instances cluster dynamical behavior is inferred from dispersed emission spectra. These cluster spectroscopic data are analyzed with a particular prejudice which is often not stated. In most cases, dynamical processes are assumed to occur in parallel. Thus, IVR and VP are competitive channels and the various IVR pathways also compete with each other.³ A cluster can thereby undergo VP or IVR into several different lower modes depending on the excitation energy. In this approach the intensity of various cluster and free molecule emissions following single vibronic level excitation of the cluster yields "branching ratios" for IVR and for VP channels. The branching ratios then lead to characterization of propensity rules with molecular chromophore modes assigned as having a "special" relationship to VP.

Several picosecond cluster studies on tetrazine(Ar)₁ and on other systems have also recently appeared in the literature.¹³⁻¹⁵ Both excited(S_1) and ground state picosecond results have been published. The excited state results indicate that IVR takes place on the time scale of a few nanoseconds.¹³ These data are consistent with a serial IVR/VP mechanism, and show qualitative agreement with calculations based on this approach.^{2(b)} We note,^{2(b)} however, that some internal inconsistencies exist between the static⁴ and time resolved¹³ tetrazine(Ar)₁ data sets which are probably attributable to interference from tetrazine(Ar)_{*n*} (*n* > 1) clusters.

The ground state picosecond data for tetrazine/argon, obtained by a three photon resonant fluorescence technique, indicate that little or no IVR occurs on the 15 ns time scale in S_0 , and are therefore in sharp contrast to the excited state times.¹⁴ This difference has been explained in terms of different chromophore-vdW mode interactions in each electronic state. These authors postulate that the extent of vibrational

coupling is indicated by the spectral bandshifts which occur upon clustering. In a later paper, these authors¹⁶ also use bandshift ideas, along with our ideas of serial relaxation dictated by energy gap laws and density of states considerations, to interpret the entire relaxation/dissociation process.

Despite the large number of studies that have been performed, the theoretical and experimental study of vibrational dynamics in vdW clusters, as represented in the literature, is currently in some disarray. In many instances neither the measurements nor the theory distinguish between IVR and VP, which are clearly different and distinct phenomena. Furthermore, very similar cluster systems have been represented and discussed by entirely distinct mechanisms. A single comprehensive mechanistic approach to these vibrational dynamics is not presently available in the literature.

In this paper we present static and time resolved spectroscopic results on the aniline(Ar)₁ and aniline(CH_4)₁ systems, which elucidate the excited state (S_1) IVR and VP dynamics. The results show that IVR and VP proceed by a serial mechanism, and that the density of vdW vibrational states is the primary factor controlling these processes in the systems studied.

II. EXPERIMENTAL

The experimental apparatus is based on a cw molecular jet and a picosecond laser/time correlated photon counting system. The molecular jet is generated by a 100 μm nozzle with a backing pressure of about 4 atm. The carrier gas is helium, with 0.2%–2.5% argon or methane, and about 10 Torr of aniline. The chamber pressure is maintained at about 10^{-5} Torr.

The laser and detection system is shown schematically in Fig. 1. It consists of a cw mode locked Nd:YAG laser (Spectra Physics model 3000) synchronously pumping a 4 MHz cavity-dumped dye laser (Spectra Physics model 375). The output is frequency doubled and focused to about 50 μm in the molecular jet for sample excitation. The laser pulse is roughly 10 ps, resulting in a coherence spectral width of about 0.5 cm^{-1} . The actual spectral width of the laser is roughly 3 cm^{-1} . The resultant emission is collected and focused through a 1 m McPherson monochromator. The detection system can be used in either of two modes; to collect time resolved emission intensities at fixed wavelengths, or to collect dispersed emission spectra by scanning the monochromator. In the time resolved mode, the monochromator is typically used in second order with a 2400 groove/mm grating. This results in considerable temporal dispersion (~ 400 ps). A 600 groove/mm grating can also be used, which results in ~ 60 ps of temporal dispersion. The detector in the time resolved mode is a Hamamatsu microchannel plate photomultiplier tube (MCP PMT) biased at 3000 V.

The subsequent time correlated single photon counting (TCSPC) electronics¹⁷ consists of two Phillips amplifiers (model 6954B-10), an H-P 8494B attenuator, a Tennelec TC 454 constant fraction discriminator (CFD), which is modified for the amplified short pulses coming from the MCP PMT, and an Ortec 457 time to amplitude converter (TAC). The reference timing pulse is provided by the out-

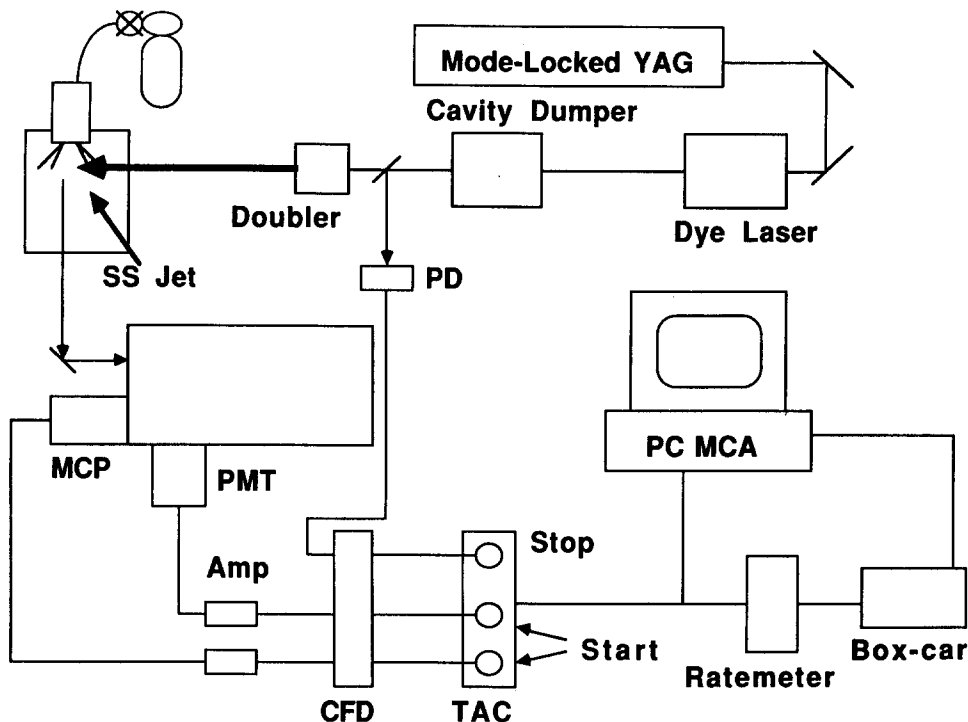


FIG. 1. Schematic diagram of the experimental apparatus. The following abbreviations are used: CFD, constant fraction discriminator; TAC, time to amplitude converter; PD, photodiode; MCP, microchannel plate photomultiplier; MCA, multichannel analyzer.

put of an H-P 4023 photodiode, which is connected to another modified channel of the constant fraction discriminator. The TAC "start" pulses are taken from the MCP PMT, and the "stop" pulses from the photodiode. The output of the TAC is put into a computer/multichannel analyzer for data storage, display and analysis. The temporal resolution of the apparatus is ~ 30 ps with the monochromator in zeroth order. Under actual data collection conditions the temporal resolution is controlled by the dispersion in the monochromator. Instrument response functions vary from 60–400 ps (fwhm) in these experiments, and are always well characterized prior to each set of experiments.

This apparatus can also be used to obtain dispersed emission spectra. In this mode, the monochromator is scanned in the second order of a 2400 groove/mm grating, and a high sensitivity gallium-arsenide photocathode PMT (Hamamatsu 943-02) is used as the detector. The PMT output is amplified by a Comlinear CLC 100 amplifier, and the same CFD and TAC detection electronics are employed as described above. Using the TAC in this way gates the detection system, essentially eliminating dark counts. The output of the TAC is connected to a ratemeter, whose output is sampled and digitized at about 10 Hz while the monochromator is scanned, giving one spectral data point per ~ 0.25 cm^{-1} . Using the apparatus in this way has the effect of counting the total number of detected photons in a 50 ns gate window for a time of 1/10 s, resulting in very high signal to noise ratio dispersed emission spectra.

The apparatus used to obtain the two color time of flight mass selected excitation spectra has been described in detail previously.¹⁰ It consists of two independently tunable nanosecond lasers, in conjunction with a 10 Hz pulsed nozzle and a time of flight mass spectrometer.

A word of caution concerning the general experimental

techniques for this research is in order. We have consistently found that the most difficult and time consuming portion of this research is not the picosecond time resolved measurements as one might naively expect. TCSPC measurements are "simply" calibrated by obtaining an accurate instrument response function on low level scattered light at regular intervals and by keeping the overall photon arrival rate below 1000 counts/s. The two most difficult aspects of these studies are the old spectroscopic problems of sample characterization and transition assignments. System characterization is especially important for these kinetic studies because the IVR/VP kinetics are strongly dependent on the size of the cluster. Thus, if IVR/VP rates in aniline(Ar)₁ are desired, the expansion system must be arranged to keep the concentration of aniline(Ar)_n ($n > 1$) clusters below the limit of detection. We find typically that for an expansion pressure of 2500 Torr of helium carrier gas, both the aniline and argon pressure should be ≤ 15 Torr. If the argon mixing pressure is increased by a factor 5 or so, distortion in both the emission spectrum and the rise and decay times of the various features is quite pronounced. Moreover, new cluster features appear in the emission spectrum of high concentration argon expansions that can be misinterpreted as arising from aniline(Ar)₁ clusters. If these argon concentration dependent features are incorrectly assumed to arise from the $n = 1$ cluster, the entire IVR/VP scheme will be misunderstood and the assigned IVR/VP lifetimes will appear to be much different than they actually are.

III. RESULTS

Figure 2 shows the two color time of flight mass selected excitation spectrum of aniline in a supersonic molecular jet. The spectrum is roughly equivalent to an optical absorption

spectrum. Several vibrational peaks, in addition to the $S_1 \leftarrow S_0$ origin, can be seen. The spectroscopy of the aniline molecule has been extensively studied, and the most intense vibronic features have been assigned.¹⁸ The assignments of some of these peaks are indicated in Fig. 2.

A. Aniline(Ar)₁

The aniline(Ar)₁ spectrum has its origin shifted about 40 cm^{-1} to the red of the corresponding bare molecule origin. The other vibronic peaks are shifted by approximately the same amount. These shifts can be understood in terms of $\sim 40 \text{ cm}^{-1}$ increase in aniline-Ar binding energy upon electronic excitation.

The dispersed emission (DE) spectrum of the aniline(Ar)₁ cluster following $\overline{0_0^0}$ excitation is shown in Fig. 3(a). (The bar over a spectral assignment indicates a cluster, rather than a bare molecule, transition.) This spectrum is very simple and, as expected, all of the observed features can be assigned to the vibrationless cluster. Figure 3(b) shows the DE spectrum following cluster excitation at 442 cm^{-1} above the $\overline{0_0^0}$ transition. The assignment of this feature is not clear and is not important for the discussion here. Emission occurs from the initially pumped cluster state, and the $\overline{0^0}$ (cluster) state. Only IVR is apparent, suggesting that the binding energy is greater than 442 cm^{-1} . Note that the aniline (Ar)₁ spectra show very little activity in the vdW modes, as can be seen from Fig. 3(a). As a result the $\overline{0_0^0}$ transition [Fig. 3(b)] remains sharp, despite the presence of 442 cm^{-1} of vibrational energy in the vdW modes.

Figure 3(c) shows that following $\overline{6a_0^1}$ excitation (494 cm^{-1}) emission appears from both the $\overline{6a_1^1}$ (cluster) and

Aniline(Ar)₁ DE

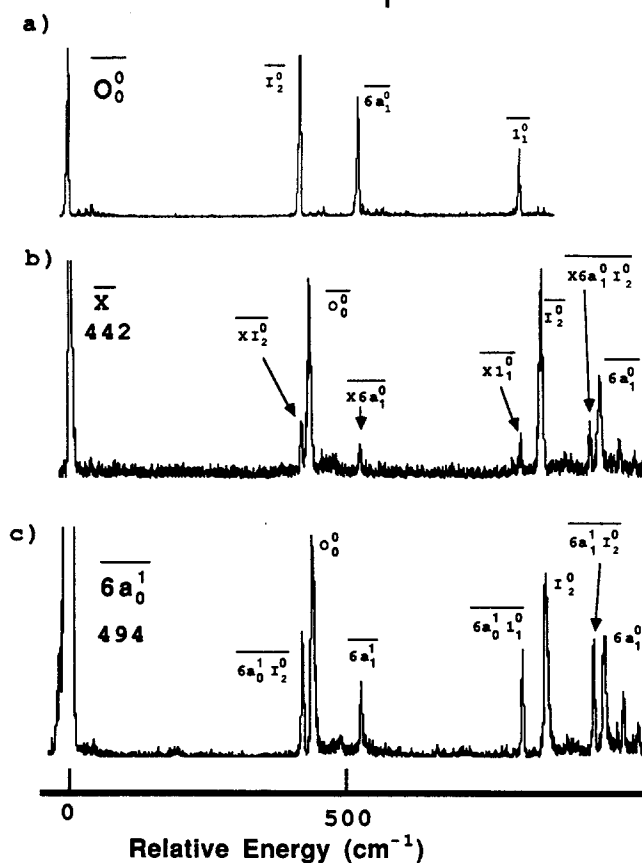


FIG. 3. Dispersed emission spectra of aniline(Ar)₁ following excitation at (a) $\overline{0_0^0}$, (b) 442 cm^{-1} , and (c) $\overline{6a_0^1}$ (494 cm^{-1}). Assignments of the more intense features are indicated. The intense peaks at 0 cm^{-1} are due partially to scattered laser excitation light.

TOFMS Aniline

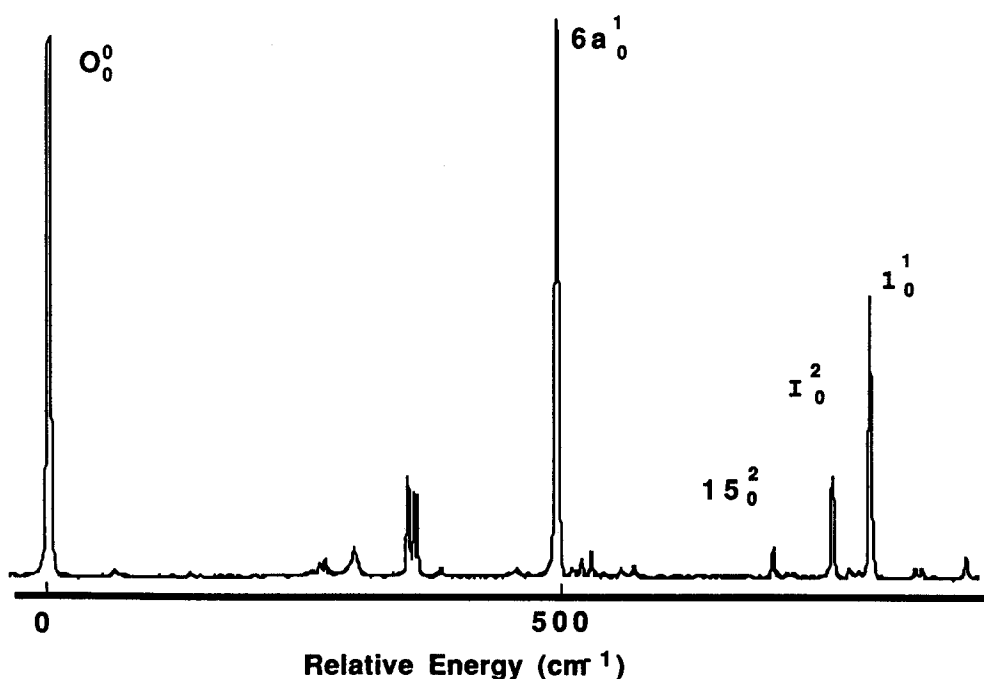


FIG. 2. Time of flight mass selected excitation spectrum of bare aniline in a molecular jet. Several of the more intense vibronic transitions are assigned.

0^0 (bare molecule) states. Thus, an upper limit of 494 cm^{-1} can be put on the excited state binding energy. Interestingly, no detectable emission is observed from the lower energy cluster states. This observation will be discussed below.

The spectra become more complicated as the excitation energy is increased. Figure 4 presents the emission spectra arising from $\overline{15}_0^2$, \overline{I}_0^2 , and $\overline{1}_0^1$ aniline(Ar)₁ cluster excitation. As the cluster excitation energy increases, more bare molecule (dissociated) vibronic states become energetically accessible, and are observed. In the case of $\overline{1}_0^1$ excitation, intense emission is observed from the $10b^1$, $16a^1$, I^1 , and 0^0 states as well as the initially pumped state. Figure 4(c) shows that all energetically possible final states are populated in approximately equal amounts (within a factor of 2 or 3).

These spectra also accurately bracket the excited state aniline(Ar)₁ binding energy. The observation of I^1 emission ($\sim 337 \text{ cm}^{-1}$ above the origin) following $\overline{1}_0^1$ excitation ($\sim 800 \text{ cm}^{-1}$ above the cluster origin) indicates that the dissociation energy is less than 460 cm^{-1} . Taken with the 442 cm^{-1} emission spectrum [Fig. 3(b)] we conclude that $442 < D_0 < 460 \text{ cm}^{-1}$.

We have also performed time resolved studies on all of the observed emission spectral features. An example of the

data typically obtained is shown in Fig. 5. This figure shows that the decay of the $\overline{6a}_1^1$ state is matched by the rise of the 0^0 state. Similar kinetics are obtained following $\overline{15}_0^2$, \overline{I}_0^2 , and $\overline{1}_0^1$ excitation. In all cases the rise times of the final (dissociated) bare molecule states are within the experimental uncertainty of the initially populated state decay times. These rise and decay times along with the relative intensities of the DE spectral lines are collected in Table I.

B. Aniline(CH₄)₁

Figure 6(a) shows the DE spectrum following $\overline{0}_0^0$ excitation of the aniline(CH₄)₁ cluster. As expected, this spectrum is very similar to the corresponding aniline(Ar)₁ spectrum; however, very different spectra and kinetics are observed in the aniline(CH₄)₁ cluster when vibrational excitation is present.

Figure 6b shows the DE spectrum arising from $\overline{6a}_0^1$ excitation of the aniline(CH₄)₁ cluster. Two types of spectral features are present: sharp peaks which originate from the vibrationless bare molecule (0^0); and a broad emission assigned to the vdW transitions built on the $\overline{0}_0^0$ band. This latter feature is very congested and broadened due to the 494

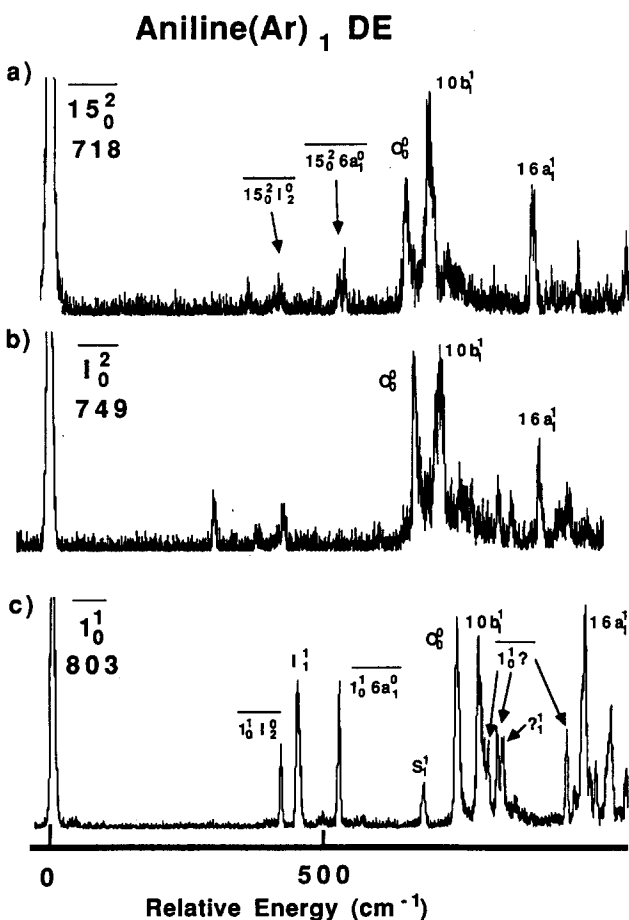


FIG. 4. Dispersed emission spectra of aniline(Ar)₁ following excitation at (a) $\overline{15}_0^2$ (718 cm^{-1}), (b) \overline{I}_0^2 (749 cm^{-1}) and (c) $\overline{1}_0^1$ (803 cm^{-1}). Assignments of the more intense features are indicated. The intense peaks at 0 cm^{-1} are due partially to scattered laser excitation light.

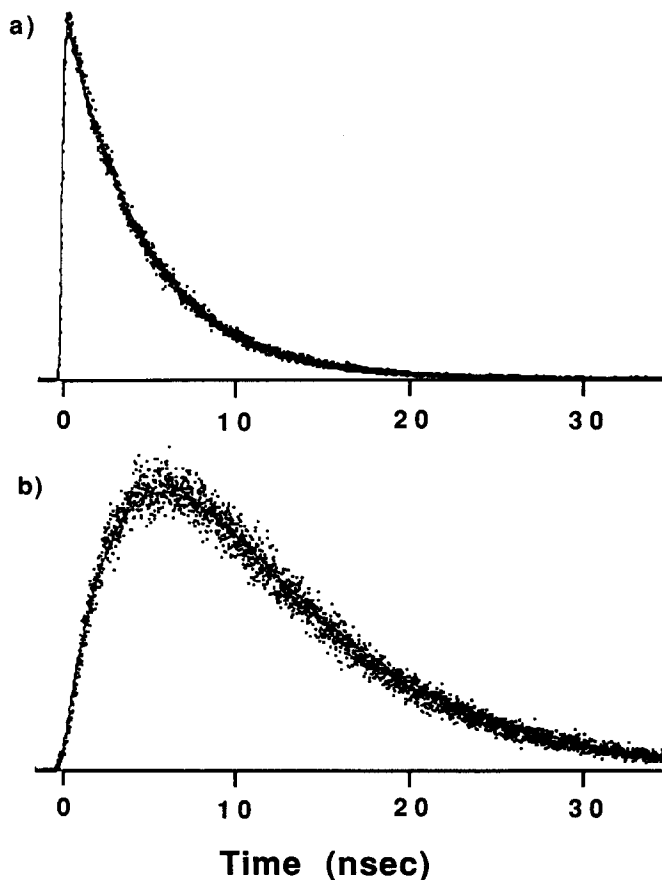


FIG. 5. Emission kinetics following $\overline{6a}_1^1$ excitation of aniline(Ar)₁. The kinetics of the $\overline{6a}_1^1 I_0^0$ and 0^0 transitions are shown. Also shown are calculated curves corresponding to (a) a 4.7 ns decay, and (b) a 4.7 ns rise and a 7.6 ns decay.

TABLE I. Aniline(Ar)₁ relative spectral intensities, rise times and decay times.^a The intensities are normalized to that of the 0₀⁰ transition. Calculated values are in parentheses.^b

Cluster excitation	Initially excited state decay times (ns)	Product state rise times ^c (ns)	Initially excited state intensity	I ¹	Product state intensities		
					16a ¹	10b ¹	0 ⁰
$\overline{6a_0^1}$	4.7(4.3)	4.7(5.2)	1.6(1.2)				1.0 (1.0)
$\overline{15_0^2}$	1.5(1.9)	1.5(2.0)	4.7(1.3)		1.0 (0.59)	1.6 (0.83)	1.0 (1.0)
$\overline{1_0^2}$	(1.7) ^d	1.0(1.8)	(0.72) ^d		0.57 (0.59)	1.0 (1.0)	1.0 (1.0)
$\overline{1_0^1}$	2.7	2.7(2.5)	1.9(1.1)	0.76 (0.11)	1.0 (0.62)	0.9 (0.72)	1.0 (1.0)

^a Measured rise and decay times are accurate to within about $\pm 10\%$.

^b Franck-Condon factors of the I₁¹, 16a₁¹, and 10b₁¹ sequence transitions are assumed to be unity.

^c Rise curves generated from the simulations are slightly nonexponential, but are similar to the fitted exponential rises.

^d Not observed.

cm⁻¹ of vibrational energy being transferred from the $\overline{6a_1^1}$ mode to the vdW modes. $\overline{6a_0^1}$ excitation of aniline(CH₄)₁ thus leads to both bare molecule 0⁰ state emission and cluster $\overline{0^0}$ emission. Figure 6(b) shows that the total (time integrated) emission intensity is about 20 times greater for the

$\overline{0^0}$ transition, than for the 0⁰ transition. The emission kinetics indicate that following $\overline{6a_0^1}$ excitation, the $\overline{0^0}$ state is long lived; about as long as following $\overline{0^0}$ excitation. Due to the spectral breadth of the $\overline{0^0}$ emission, it has considerable overlap with the sharp 0⁰ peak. As a result, clean emission kinetics for the 0⁰ transition cannot be obtained. No emission is identified from the initially excited state (i.e., $\overline{6a_1^1}$, etc.). These results are in stark contrast to those found for the aniline(Ar)₁ cluster.

Figure 6(c) shows the DE spectrum which results following $\overline{15_0^2}$ excitation of the aniline(CH₄)₁ cluster. Two types of spectral features are observed: 0⁰ and (much weaker) $\overline{0^0}$ transitions. The relative intensity of $\overline{0^0}$ band is found to increase upon increasing the CH₄/He ratio (i.e., from 0.2% to 2.0%) in the expansion gas mixture. Thus, we conclude that much of this emission is a result of excitation of aniline(CH₄)_n (*n* > 1) clusters. From the DE spectra observed following $\overline{6a_0^1}$ excitation we conclude that the aniline(CH₄)₁ excited state binding energy is less than 494 cm⁻¹ and that the bare molecule 10b¹ and 16a¹ states are thus energetically accessible from the $\overline{15^2}$ state. Emission from these states is totally absent in the observed spectrum. Again we emphasize the difference between the aniline(Ar)₁ and aniline(CH₄)₁ spectra. Also, no emission from the initially excited $\overline{15^2}$ state can be detected. The very high signal to noise ratio permits the detection of very short lived, and therefore very weak spectral features. Thus, this observation indicates that the initially excited state has a lifetime of less than about 100 ps. Figure 7 shows the 0⁰ emission kinetics following $\overline{15_0^2}$ excitation. The rise time of the 0⁰ state is 240 ± 50 ps. The obvious question of what intermediate states are populated arises from the disparity of these rise and decay times. The most likely candidate for an intervening state in the kinetic IVR/VP process is $\overline{0^0}$. This suggestion is based on the observation that the only intermediate state seen following $\overline{6a_0^1}$ excitation is $\overline{0^0}$. When a considerable amount of energy is in the vdW modes, the DE peaks are

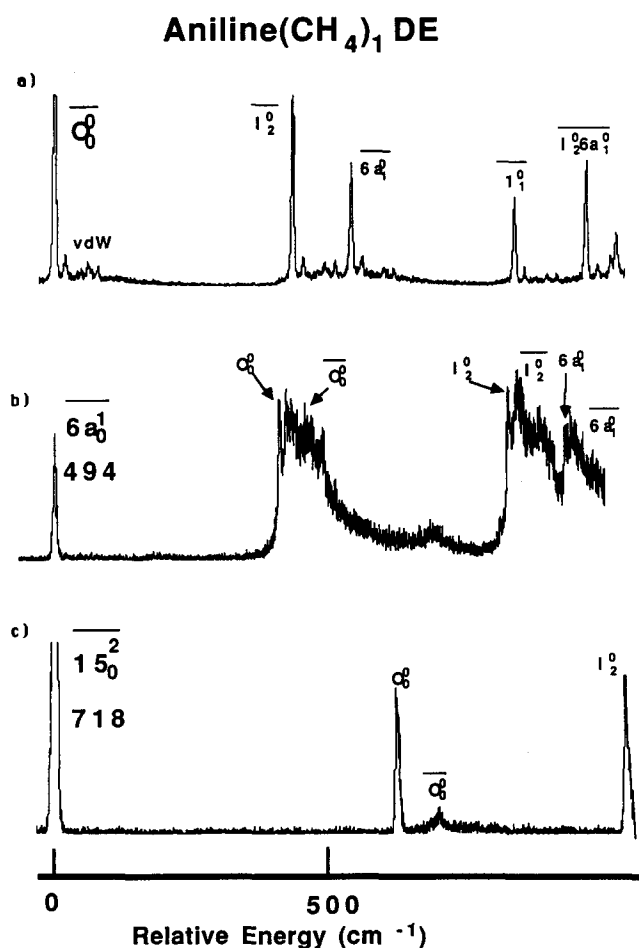


FIG. 6. Dispersed emission spectra of aniline(CH₄)₁ following excitation at (a) 0₀⁰, (b) $\overline{6a_0^1}$ (494 cm⁻¹), (c) $\overline{15_0^2}$ (718 cm⁻¹). Assignments of the more intense features are indicated. The intense peaks at 0 cm⁻¹ are due partially to scattered laser excitation light.

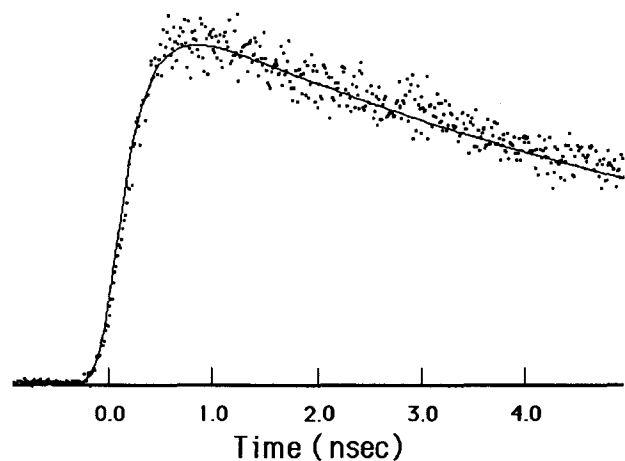


FIG. 7. Emission kinetics following $\overline{15}_0^2$ excitation of aniline(CH_4)₁. The kinetics of the 0^0 transition are shown. Also shown is a calculated curve corresponding to the convolution of the instrument response function with a 240 ps rise and a 7.6 ns decay.

very broad, as in the case of the $\overline{0}_0^0$ emission following $\overline{6a}_0^1$ excitation [Fig. 6(b)]. Therefore, any $\overline{0}_0^0$ emission following $\overline{15}_0^2$ excitation would also be expected to be quite broad. This breath, in combination with the relatively short lifetime (~ 240 ps), would make intermediate (cluster) state emission difficult to detect. Note too that the broad $\overline{0}_0^0$ emission may also slightly contaminate the 0^0 emission kinetics, which would result in a component of emission which has a fast rise time. The actual rise time of the 0^0 state may therefore be slightly longer than the observed 240 ps. Thus, the $\overline{0}^0$ cluster state may well be populated by IVR from the $\overline{15}_0^2$ state in less than 100 ps, and may live for about 240 ps prior to VP. The above spectral and kinetic results for aniline(CH_4)₁ are collected in Table II.

Finally, DE spectra and emission kinetics following $\overline{6a}_0^1 + \text{vdW}$ excitation at $\overline{0}_0^0$ plus 506 cm^{-1} and $\overline{0}_0^0$ plus 518 cm^{-1} have also been observed. Due to the weakness of these features, acceptable signal to noise ratios are very difficult to obtain. Excitation at $\overline{0}_0^0$ plus 506 cm^{-1} yields spectra and kinetics which are clearly contaminated from higher aniline(CH_4)_n clusters and perhaps hot bands, as multiexponential decays are observed. The $\overline{0}_0^0$ plus 518 cm^{-1} feature yields spectra and kinetics which are qualitatively similar to and intermediate between those for $\overline{6a}_0^1$ and $\overline{15}_0^2$

excitation. A quantitative interpretation of these preliminary results is not currently possible: problems associated with interference from other clusters and hot bands must be resolved before these interesting results can be fully analyzed. We are presently investigating the DE spectra and kinetics of aniline(X)₁ clusters upon chromophore plus vdW mode excitation.

IV. DISCUSSION

The most striking feature of our experimental results is that the aniline(Ar)₁ cluster dissociates into all energetically accessible vibrational levels of the bare molecule, whereas the aniline(CH_4)₁ cluster dissociates only to the vibrationless level of the bare molecule. No plausible explanation for this difference in dynamical behavior can be found within the framework of a parallel IVR/VP mechanism.

That data can be understood in terms of a serial IVR/VP model. In this model chromophore to vdW mode IVR precedes VP. Once the amount of energy in the vdW modes exceeds the binding energy, either of two processes can occur: further chromophore to vdW mode IVR, or VP. The VP rate is determined by the amount of energy in the vdW modes; the VP rate is therefore time dependent and varies with the extent of IVR. The observed spectra and kinetics for both aniline(Ar)₁ and aniline(CH_4)₁ clusters systems will be the result of a competition between these two processes. The general theme for rationalizing the aniline(Ar)₁ and aniline(CH_4)₁ data is as follows: for the aniline(Ar)₁ cluster, IVR is very slow, due in part to the low density of vdW mode receiving states, and VP is very fast, because of the small (three mode) vdW phase space. For the aniline(CH_4)₁ cluster, IVR is very fast, due in part to the high density of vdW mode receiving states, and VP is relatively slow, because of the larger (six mode) vdW phase space.

We now consider each individual component of the overall redistribution/dissociation (cluster to bare molecule) process, and propose a simple model to understand the observed results. The chromophore to vdW mode IVR in this model is simply given by the Fermi golden rule transition probability expression: the product of a matrix element squared times a density of final receiving states. The rate of chromophore to vdW mode IVR should then be given by a product of three terms: a coupling coefficient between chromophore and vdW mode (initial and final) states; a vibrational wave function overlap term for initial and final vdW

TABLE II. Aniline(CH_4)₁ relative spectral intensities, rise times, and decay times. The intensities are normalized to that of the 0^0 transition. Calculated values are in parentheses.

Cluster excitation	Initially excited decay times (ns)	Product state rise times (ns)	Initially excited state intensity	Product state intensity ^a	
				$\overline{0}^0$	0^0
$\overline{6a}_0^1$	<0.1 (10^{-3})	(160)	0(0)	20 (20)	1.0 (1.0)
$\overline{15}_0^2$	<0.1 (10^{-3})	0.24(0.18)	0(0)	0 (0)	1.0 (1.0)

^a States not identified have zero calculated and observed intensity.

mode states; and the density of final vdW vibrational receiving states.

While the above ideas have not been previously applied to the problem of chromophore to vdW mode IVR, they are not without precedent. The first two terms lead to a general "energy gap law" for IVR, in which the exchange of many quanta of energy between the chromophore and vdW modes is not favored. Analogous models have also been applied to the direct dissociation of diatomic(He)₁-type clusters.¹⁹ This situation is somewhat analogous to vibrational relaxation of small and medium sized molecules in rare gas matrices, for which the coupling of the molecular vibrations to the matrix phonons are also fairly weak, and energy gap laws characterize the relaxation rates.^{1,20} The VP rate constants in this model can be estimated for any given amount of energy placed in the vdW modes by IVR. The calculations are based upon a restricted (to the vdW mode phase space) RRKM theory.

The qualitative results of this model can be readily calculated: differences in the predicted behavior of aniline(Ar)₁ and aniline(CH₄)₁ are both striking and at the same time in agreement with the observed results. Aniline(CH₄)₁ has six degrees of freedom in the vdW modes; one stretch, two bends and three hindered rotations. In contrast, aniline(Ar)₁ has only the stretch and bend degrees of freedom. This results in very different densities of states for these complexes. The density of vibrational states at any given energy $N(E)$ can be estimated (see below). For aniline(CH₄)₁ at 700 cm⁻¹ of energy $N(E) = 3 \times 10^4$ states cm⁻¹, whereas for aniline(Ar)₁ at the same energy, $N(E) \approx 15$ states cm⁻¹. Thus, the density of vdW vibrational states is about 10³ greater for aniline(CH₄)₁ at 700 cm⁻¹ of energy.

Consider now how this density of states difference can affect the IVR rates for aniline clusters: IVR should be much faster in the aniline(CH₄)₁ system than in the aniline(Ar)₁ system. IVR rates are measured to be on the order at a few nanoseconds in the aniline(Ar)₁ system and if the coupling constants are comparable for both systems, IVR rates for aniline(CH₄)₁ will be three orders of magnitude faster than those measured for aniline(Ar)₁—a few picoseconds.

The VP rate for aniline(Ar)₁ with 700 cm⁻¹ of energy in the vdW modes and a binding energy at 450 cm⁻¹, can be calculated by RRKM theory, and is about (5 ps)⁻¹. Thus, in the case of aniline(Ar)₁ chromophore to vdW IVR is slow and rate limiting, and subsequent VP is very fast. Any IVR process which puts energy in excess of the binding energy into the vdW modes is immediately followed by VP. All of the lower chromophore levels are populated by IVR, and as a result, the bare molecule is formed in all of the energetically accessible states. This model predicts that IVR will be the overall rate controlling process for aniline(Ar)₁ dissociation.

Very different VP kinetics are predicted for the aniline(CH₄)₁ case. Here we find that with 700 cm⁻¹ of energy in the vdW modes and a 480 cm⁻¹ binding energy, the VP rate is about (180 ps)⁻¹. Thus, in sharp contrast to the aniline(Ar)₁ case, IVR in aniline(CH₄)₁ is very fast compared to VP. IVR is expected to populate all the lower chromophore levels just as in the aniline(Ar)₁ case; however, in

the aniline(CH₄)₁ case subsequent IVR to the $\bar{0}^0$ level is complete before VP can occur. Finally, VP occurs relatively slowly from $\bar{0}^0$ and is the rate limiting step in the entire process. This model predicts that formation of the bare vibrationless molecule will be limited by the rate of VP for aniline(CH₄)₁, and will be on the hundreds of picoseconds to nanoseconds time scale. All of the above qualitative predictions of this model are borne out by the experimental results.

We have performed detail quantitative numerical simulations based on the above qualitative ideas. In these calculations, the probability of an IVR transition from chromophore state j to state i , P_{ij} , is given by $P_{ij} = (C_{ij}) \times (\text{energy gap term}) \times (\rho_i)$, in which ρ_i is the density of vdW states at the energy $(E_{\text{exc}} - E_i)$. The quantity $(E_{\text{exc}} - E_i)$ is the total vibrational energy minus the vibrational energy remaining in the chromophore modes, and hence is the amount of vibrational energy in the vdW modes following the IVR transition. The coupling coefficients C_{ij} for any set of initial and final chromophore states and the exact functional form of the energy gap law are difficult to determine. Both depend upon the details of the potential surface. Nonetheless, some reasonable approximations can be made which result in a phenomenological theory of IVR. The notion of partitioning the vibrational phase space into chromophore and vdW regions is based on the observation that the vdW mode frequencies are much lower than the chromophore mode frequencies. The comparatively slow chromophore to vdW energy transfer is due to part of this frequency mismatch. This suggests that the coupling constant C_{ij} should be inversely proportional to ν_i and ν_j , the chromophore vibrational frequencies.

Energy gap laws, based on wave function overlaps, have been worked out for a variety of situations. The functional form of the energy gap term depends on the nature of the final states. For example, small molecules in rare gas matrices undergo vibrational relaxation to the librational and/or hindered rotational degrees of freedom. In this case, the energy gap term has the functional form $\exp(-\sqrt{\Delta E})$, in which ΔE is the amount of energy transferred.^{1,20} Librational motion in a low temperature matrix may be somewhat analogous to bending motions for cluster vdW modes. Based on this rather loose analogy, a similar form can be adopted for chromophore to vdW more energy transfer.

The density of the vdW vibrational states is easily evaluated, if the vdW mode energies are either known or if reasonable guesses concerning their energies and anharmonicities can be made. Thus, the matrix of IVR rates can be constructed with a single adjustable parameter which scales all the IVR rates.

With the above assumptions and approximations, numerical simulations of the IVR/VP process can be performed. Two population vectors, N_c and N_{nc} are defined. $N_c(i)$ is the cluster population with the chromophore in the i th vibrational level and similarly, $N_{nc}(i)$ refers to bare molecule populations. To calculate the time evolution of the population vectors three matrices must be defined: \mathbf{P} is the IVR transition probability matrix with matrix elements P_{ij} for the chromophore transition to level i from level j in a time interval Δt ; \mathbf{K} is the VP matrix; and \mathbf{R} is the radiationless

transition matrix. Then

$$R_{ij} = (1 - k_{isc+ic} \Delta t) \delta_{ij},$$

$$K_{ij} = (1 - k_i \Delta t) \delta_{ij},$$

$$P_{ij} = \frac{A}{\nu_j} \exp(-\sqrt{\Delta E_{ij}}) \rho_i$$

in which k_{isc+ic} is the rate constant for internal conversion ($S_1 \rightarrow S_0$) and intersystem crossing ($S_1 \rightarrow T_1$) for aniline, and k_i is the RRKM unimolecular reaction (dissociation) rate constant characteristic of an energy ($E_{exc} - E_i$) in the vdW modes (see below). A is the only adjustable parameter of the model, which temporally scales the entire IVR process. The temporal evolution of the population vectors is given by

$$N_c(t + \Delta t) = \mathbf{RKP} N_c(t)$$

and

$$N_{nc}(t + \Delta t) = \mathbf{RN}_{nc}(t) + (1 - \mathbf{K})N_c(t).$$

The RRKM rate constant $k_i = k(E)$ can easily be calculated using the Marcus Rice approximation,^{2(a)}

$$k(E) = \frac{1}{h} \frac{\sum P(E^+)}{N(E)}$$

with

$$N(E) \approx \frac{e^{S-1}}{(S-1)! \Pi h \nu_i}$$

and

$$\sum P(E^+) \approx \frac{(E^+)^{S-1}}{(S-1)! \Pi h \nu_i}$$

in which $\sum P(E^+)$ is the sum of vibrational states above the dissociation energy excluding the reaction coordinate, $E^+ = E - E_0$ with E_0 the cluster binding energy, $N(E)$ is the total vibrational density of states at energy E , ν_i is the vdW mode energy, and S is the number of degrees of freedom of the vdW modes. The prime on the product sign indicates exclusion of the reaction coordinate. The assumption made in these calculations is that the cluster transition state is a "tight binding" one.²¹ The calculation of RRKM rates is explained in detail in Refs. 2(a) and 21.

The IVR rates in the aniline(Ar)₁ case are rather sensitive to the densities of states. In this case, the values of ρ_i [$= N(E)$] used in the construction of the IVR transition probability matrix are calculated with a direct count method.²² Vibrational frequencies of 45 cm⁻¹ (stretch), and 15 cm⁻¹ (both bends) and anharmonicities of 3% (i.e., $\Delta \nu_{i,i+1} / \Delta \nu_{i-1,i} = 0.97$) are assumed.

Quantitative predictions of the model can be made from the simulation procedure described above. The results of these simulations, in terms of kinetics and spectral quantum yields, are compared with the experimental results in Tables I and II. In all cases the agreement is quite good; within a factor of about two.

Several comments and observations about these calculations and their comparison to the experimental data can be made. The experimental results show that the extent of vdW vibrational overlap tends to decrease with increasing energy

change in an IVR transition. This can be seen from the results in Table I. For example, following aniline(Ar)₁ $\overline{1}_0^1$ excitation, the 0^0 , $10b^1$, $16a^1$, and I^1 final product states are formed in approximately the same amounts. If the vibrational overlap were energy independent, then the 0^0 state would be somewhat favored due to the higher density of vdW states corresponding to that level. Energy gap laws are simply generalizations of how vibrational overlaps vary with the energy difference between states. The functional form of the energy gap law used is chosen rather arbitrarily—basically large energy chromophore transitions are not favored.

The assumed energy gap law, in combination with the calculated density of vdW states, determines the calculated energy dependence of IVR transition rates. The calculations predict that for aniline(Ar)₁ IVR from the initially excited state is far slower than subsequent IVR transitions. Thus, the calculated final state rise times closely match the initially excited state decay times, in agreement with the experimental results.

VP is predicted to be the rate limiting process for aniline(CH₄)₁. The calculated VP rate for $\overline{6a}^1_0$ excitation depends strongly on the assumed binding energy E_0 . With an assumed E_0 of 480 cm⁻¹ the calculated $\overline{6a}^1$ VP rate is (160 ns)⁻¹. The vast majority of emission would be from the cluster $\overline{0}^0$ state and not the bare molecule 0^0 state, in agreement with the observations. The calculated VP rate for $\overline{15}^0_0$ excitation is 100 ps, again in good agreement with the experimental results.

The most severe approximation in this calculation is that the IVR transition matrix \mathbf{P} is scaled by a single constant coupling parameter for all modes. This approximation is surely not completely correct; however, the agreement between the experimental and calculated results suggests that this approximation is good to within a factor of about 2.

Finally, a comment on the overall description of the dissociation process is in order. In the aniline(CH₄)₁ case, chromophore to vdW mode IVR is very fast and VP is the rate controlling process. Thus, both restricted (considering only the vdW mode phase space) and unrestricted or simple (considering both vdW and chromophore mode combined phase space) RRKM theories give the same correct dissociation rate. In the aniline(Ar)₁ case, however, IVR is quite slow and it becomes the rate controlling process rather than VP. As we have pointed out above, IVR rates depend on coupling coefficients, density of final receiving states, the amount of energy transferred between chromophore and vdW modes, etc. Consequently, the overall dissociation rate for aniline(Ar)₁ is much slower than the simple unrestricted RRKM calculation; in fact, the overall dissociation time (the time between photon absorption and cluster dissociation) for this cluster is unrelated to any RRKM or other statistical unimolecular reaction rate mechanism. Indeed, Table I demonstrates that the total aniline(Ar)₁ dissociation rates do not increase monotonically with excitation energy. The kinetics for aniline(Ar)₁ dissociation could thereby be called an example of "non-RRKM" or "mode specific" behavior. We believe that such a description is misleading and obscures the physical picture because once ener-

gy has been transferred from the chromophore modes to the vdW modes, the dissociation process is indeed a statistical one. That is, IVR amongst the vdW modes is rapid compared to any other kinetics and VP in both clusters can be described by a restricted statistical RRKM model.

V. CONCLUSIONS

The main conclusions of this work can be summarized as follows:

(1) Aniline(Ar)₁ and aniline(CH₄)₁ clusters exhibit much different S₁ vibrational dynamics. Aniline(Ar)₁ undergoes IVR relatively slowly (nanoseconds), and all energetically accessible bare molecule states are populated by VP. In contrast, aniline(CH₄)₁ undergoes rapid IVR (< 100 ps) and only the 0⁰ level is populated by VP from 0⁰.

(2) The dynamical differences between aniline(Ar)₁ and aniline(CH₄)₁ can be understood in terms of a serial IVR/VP model. In this model, the rate of IVR is given by Fermi's golden rule, and the rate of VP is given by a restricted RRKM theory with regard to both IVR and VP processes.

(3) The density of vdW vibrational states is the single most important factor of determining the dynamical differences between aniline(Ar)₁ and aniline(CH₄)₁.

ACKNOWLEDGMENT

This work was supported in part by grants from NSF and ONR.

¹ (a) P. Avouris, W. M. Gelbart, and M. A. El-Sayed, *Chem. Rev.* **77**, 793 (1977); (b) S. Mukamel, *J. Phys. Chem.* **89**, 1077 (1985); (c) S. Mukamel and J. Jortner, *Excited States*, edited by E. C. Lim, (Academic, New York, 1977), Vol. III, p. 57.

² (a) D. J. Robinson and K. A. Holbrook, (*Unimolecular Reactions*, Wiley, New York, 1972); (b) D. F. Kelley and E. R. Bernstein, *J. Phys. Chem.* **90**, 5164 (1986); (c) J. I. Steinfeld, J. S. Francisco, and W. L. Hase, *Chemical Kinetics and Dynamics* (Prentice Hall, New York, 1989); (d) R. D. Levine and R. B. Bernstein, *Molecular Reaction Dynamics and Chemical Reactivity*, (Oxford, Oxford, 1987).

³ (a) J. A. Beswick and J. Jortner, *Adv. Chem. Phys.* **47**, 363 (1981), and references therein; (b) S. H. Lin, *Radiationless Transitions* (Academic, New York, 1980).

⁴ (a) D. V. Brumbaugh, J. E. Kenny, and D. H. Levy, *J. Chem. Phys.* **78**, 3415 (1983), and references therein; (b) C. A. Haynam, D. V. Brumbaugh, and D. H. Levy, *ibid.* **80**, 2256 (1984); (c) Y. D. Park and D. H. Levy, *ibid.* **81**, 5527 (1984).

⁵ C. A. Haynam, L. Young, C. Morter, and D. H. Levy, *J. Chem. Phys.* **81**, 5216 (1984).

⁶ N. Mikami, Y. Scigobora, and M. Ito, *J. Phys. Chem.* **90**, 2080 (1986); H. Abe, Y. Okyanagi, M. Iokijo, N. Mikami, and M. Ito, *ibid.* **89**, 3512 (1985).

⁷ N. Halberstadt and B. Soep, *Chem. Phys. Lett.* **87**, 109 (1982); *J. Chem. Phys.* **80**, 2340 (1984).

⁸ (a) T. A. Stephensen, P. L. Radloff, and S. A. Rice, *J. Chem. Phys.* **81**, 1060 (1984); (b) T. A. Stephensen and S. A. Rice, *ibid.* **81**, 1083 (1984).

⁹ (a) C. S. Parmenter, *J. Phys. Chem.* **86**, 1735 (1982); (b) K. W. Butz, D. L. Catlett, G. E. Ewing, D. Krajnovich, and C. S. Parmenter, *J. Chem. Phys.* **90**, 3533 (1986); (c) H. K. O, C. S. Parmenter, and M. C. Su, *Ber. Bunsenges, Phys. Chem.* **92**, 253 (1988).

¹⁰ (a) E. R. Bernstein, K. Law, and M. Schauer, *J. Chem. Phys.* **80**, 107, 634 (1984); (b) M. Schauer, K. Law, and E. R. Bernstein, *ibid.* **81**, 49 (1984); (c) M. Schauer, K. Law, and E. R. Bernstein, *ibid.* **82**, 726, 736 (1985).

¹¹ D. O. DeHaan, A. L. Holton, and T. S. Zwier, *J. Chem. Phys.* **90**, 3952 (1989).

¹² (a) R. E. Miller, *J. Phys. Chem.* **90**, 3301 (1986); (b) D. J. Nesbitt, *Chem. Rev.* **88**, 843 (1988).

¹³ (a) J. J. F. Ramackers, J. Langelaar, and R. P. H. Rettschnick, *Picosecond Phenomena III*, edited by K. Eisenthal, R. M. Hochstrasser, W. Kaiser, and A. Laubereau (Springer, Berlin, 1982), p. 264, (b) M. Heppener, A. G. M. Kunst, D. Bebelaar, and R. P. H. Rettschnick, *J. Chem. Phys.* **83**, 5314 (1985); (c) M. Heppener and R. P. H. Rettschnick, in *Structure and Dynamics of Weakly Bound Molecular Complexes*, edited by A. Weber, (Reider, Dordrecht, 1987), p. 553; (d) J. J. F. Ramackers, L. B. Krijnen, H. J. Lips, J. Langelaar, and R. P. H. Rettschnick, *Laser Chem.* **2**, 125 (1983); (e) J. J. F. Ramackers, H. K. van Dijk, J. Langelaar, and R. P. H. Rettschnick, *Faraday Discuss. Chem. Soc.* **75**, 183 (1983).

¹⁴ (a) P. M. Weber and S. A. Rice, *J. Chem. Phys.* **88**, 1082, 6107, 6120 (1988); (b) B. A. Jacobsen, S. Humphrey, and S. A. Rice, *ibid.* **89**, 5624 (1988).

¹⁵ D. H. Semmes, J. S. Baskin, and A. H. Zewail, *J. Am. Chem. Soc.* **109**, 4104 (1987).

¹⁶ P. M. Weber and S. A. Rice, *J. Phys. Chem.* **92**, 5470 (1988).

¹⁷ G. R. Fleming, *Chemical Applications of Ultrafast Spectroscopy* (Oxford, Oxford, 1986); *Adv. Chem. Phys.* **49**, 1 (1982), and references therein.

¹⁸ D. A. Chernoff and S. A. Rice, *J. Chem. Phys.* **70**, 2521 (1979), and references therein

¹⁹ G. E. Ewing, *J. Phys. Chem.* **91**, 4662 (1987).

²⁰ V. E. Bondybey and L. E. Brus, *Adv. Chem. Phys.* **41**, 269 (1980).

²¹ D. M. Wardlaw and R. A. Marcus, *Chem. Phys. Lett.* **110**, 230 (1984); *Adv. Chem. Phys.* **70**, 231 (1987).

²² S. E. Stein and B. S. Rabinovitch, *J. Chem. Phys.* **58** 2438 (1973).